BIOCONVECTIVE STUDY OF SECOND GRADE NANOFLUID OVER ELONGATED SHEET

Afsar Hossain Sarkar, Dr. Annapurna Ramakrishna Sinde
Department of Mathematics, Dr. A.P.J. Abdul Kalam University, Indore, M.P., India

ABSTRACT:
The study of non-Newtonian fluid power and mass trade has been expanded due to their applications in science, for example, metallurgical cycle, polymer ejection, glass blowing, diamond creation, and so on. Several scholars have expressed interest in the cutoff layer stream of a non-Newtonian sticky fluid. At high temperatures, the MHD stream issue in the presence of warm radiation has become more essential in industry. As a result, information on the radiation heat motion becomes critical. This paper reflects Bioconvective Study of Second Grade Nanofluid Over Elongated Sheet.

KEYWORDS: fluid, radiation, diamond, essential, absorb, heat
DOINumber:10.48047/nq.2022.20.22.NQ10424 **NeuroQuantology2022;20(22):4254-4267**

1. LITERATURE REVIEW

Yin [1] presented the magnetohydrodynamic convection flow over a non-isothermal wedge. In general, microorganisms exhibit greater carbon dioxide retention than plants. Bioconvection represents an unstructured model formed in a suspension by slightly denser microorganisms compared to those that vertically swim in water. Due to this accumulation of microorganisms, the upper surface becomes notably dense and substantial, making it easy to deplete. Bioconvection finds various applications, such as in food processing, bioreactors, wine production, bio-diesel fuels, and fuel cell development. Recognizing its significance, Guell et al. [2] and Hillesdon et al. [3] initiated studies on bioconvection flows in the 1980s and 1990s, respectively. Subsequent studies by several authors have aimed to provide further insights into bioconvection, as documented in [4-5]. Kuznetsov [6] later developed a numerical model for bioconvection considering porous media. He found that various factors, including cell deposition, influence bioconvection's progression. More recently, Raju and Sandeep [7] analyzed the flow characteristics over a rotating cone/plate with bioconvection, highlighting the role of rotation in controlling the flow. Nadeem and Lee [8] investigated magnetohydrodynamic flow over a bidirectional stretching sheet using a power series solution and noted that the magnetic field enhances the velocity field. Hussain et al. [9] studied the flow over a rotating channel containing carbon nanotubes. Akbar et al. [10] examined magnetohydrodynamic natural convection flow over a stretching surface laden with nanoparticles, concluding that the nanoparticle volume fraction further improves the heat transfer rate. Raju and Sandeep [11] studied magnetohydrodynamic Carreau fluid flow over a wedge with cross-diffusion effects, showing how cross-diffusion influences power and mass transfer characteristics. Recently, the homotopy analysis of linear operator equations using the modified operator method was explored by Hussain et al. [12] and Nadeem et al. [13] analyzed stagnation point flow loaded with various nanoparticles.

The aim of this current study is to investigate the influence of thermophoresis and thermal radiation on power and mass transfer of a second-grade fluid past an infinite stretching sheet with convective surface heat flux under the influence of a magnetic field and chemical reaction.

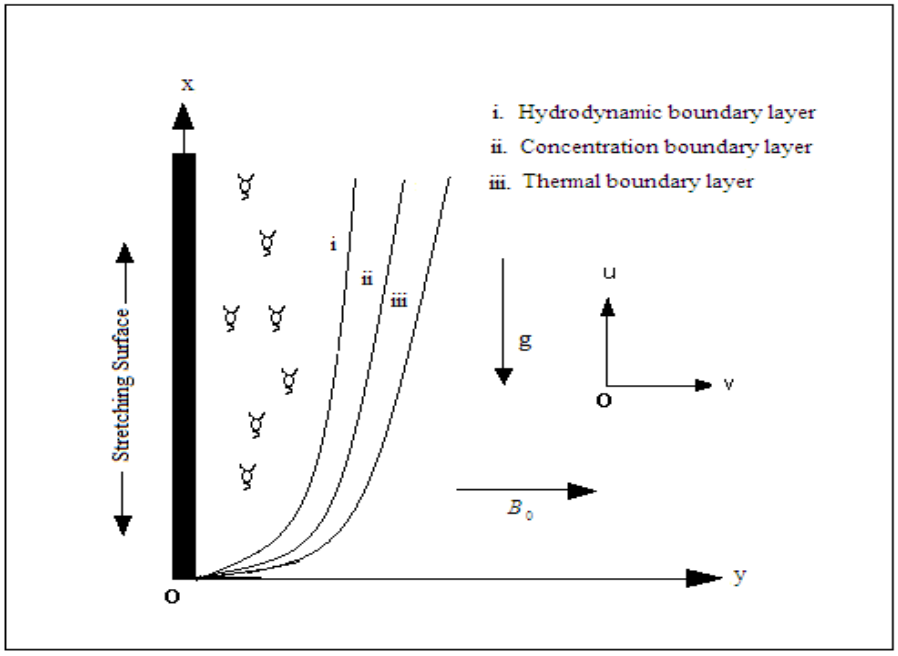

Figure 1: Physical model of the flow

2. MATHEMATICAL FORMULATIONS

Consider the boundary layer flow of an incompressible and electrically conducting second-grade fluid over an expanding sheet aligned with the plane y=0, with the flow being confined to y>0. This scenario involves viscous dissipation and Joule heating. The flow is induced by the expansion of the sheet, caused by the simultaneous action of two equal and opposite forces along the x-axis. The sheet's expansion velocity is given by uw(x) = ax, where 'a' is a constant and 'x' is the direction measured along the expanding surface from the origin. In this study, thermal radiation is occurring within the flow, and the impact of thermophoresis is being considered to enhance the understanding of mass transfer near the surface. A uniform transverse magnetic field with strength B0 is applied in the y-direction. The expanding surface is maintained at a constant temperature Tw, which is higher than the steady temperature T8 of the surrounding fluid. Due to the boundary layer behavior, the temperature gradient along the y-direction is significantly greater than that along the x-direction. As a result, the thermophoretic velocity component normal to the surface becomes noteworthy.

Given these assumptions, the boundary layer conditions for the transient second-grade fluid flow can be expressed as described by Olajuwon [14] and Das [15].

$$\left.\begin{aligned}
&\frac{\partial \mathrm{u}}{\partial \mathrm{x}}+\frac{\partial \mathrm{v}}{\partial \mathrm{y}}=0\\
&\mathrm{u}\frac{\partial \mathrm{u}}{\partial \mathrm{x}}+\mathrm{v}\frac{\partial \mathrm{v}}{\partial \mathrm{y}}=\nu\frac{\partial^2 \mathrm{u}}{\partial \mathrm{y}^2}+\frac{\alpha_1}{\rho}\left[\frac{\partial}{\partial \mathrm{x}}(\mathrm{u}\frac{\partial^2 \mathrm{u}}{\partial \mathrm{y}^2})-\frac{\partial \mathrm{u}}{\partial \mathrm{y}}\frac{\partial^2 \mathrm{u}}{\partial \mathrm{x}\partial \mathrm{y}}+\mathrm{v}\frac{\partial^3 \mathrm{u}}{\partial \mathrm{y}^3}\right]\\
&-\frac{\sigma \mathrm{B}_0^2 \mathrm{u}}{\rho}+g\beta(\mathrm{T}-\mathrm{T}_\infty)+g\beta^*(\mathrm{C}-\mathrm{C}_\infty)\\
&\rho \mathrm{c}_\mathrm{p}\left(\mathrm{u}\frac{\partial \mathrm{T}}{\partial \mathrm{x}}+\mathrm{v}\frac{\partial \mathrm{T}}{\partial \mathrm{y}}\right)=\kappa\frac{\partial^2 \mathrm{T}}{\partial \mathrm{y}^2}+\tau\left\{D_{BM}\frac{\partial C}{\partial y}\frac{\partial T}{\partial y}+\frac{D_{TP}}{T_\infty}\left(\frac{\partial T}{\partial y}\right)^2\right\}\\
&-\frac{\partial \mathrm{q}_\mathrm{r}}{\partial \mathrm{y}}+\mu\left(\frac{\partial \mathrm{u}}{\partial \mathrm{y}}\right)^2+\alpha_1\frac{\partial \mathrm{u}}{\partial \mathrm{y}}\left[\frac{\partial}{\partial \mathrm{y}}\left(\mathrm{u}\frac{\partial \mathrm{u}}{\partial \mathrm{x}}+\mathrm{v}\frac{\partial \mathrm{u}}{\partial \mathrm{y}}\right)\right]+\sigma {B_0}^2 u^2\\
&\mathrm{u}\frac{\partial \mathrm{C}}{\partial \mathrm{x}}+\mathrm{v}\frac{\partial \mathrm{C}}{\partial \mathrm{y}}=D_{BM}\frac{\partial^2 C}{\partial \mathrm{y}^2}+\frac{D_{TP}}{T_\infty}\frac{\partial^2 \mathrm{T}}{\partial \mathrm{y}^2}-\frac{\partial(\mathrm{V}_\mathrm{T}\mathrm{C})}{\partial \mathrm{y}}-\mathrm{k}_\mathrm{r}(\mathrm{C}\text{-}\mathrm{C}_\infty)\\
&u\frac{\partial M}{\partial x}+v\frac{\partial M}{\partial y}=D_{MO}\frac{\partial^2 M}{\partial y^2}-\left(\frac{bW_c}{\Delta C}\right)\frac{\partial}{\partial y}\left(M\frac{\partial C}{\partial y}\right)
\end{aligned}\right\} \quad \text{.....(1)}$$

Here the speed parts along x, y-hub are u, v separately, g is the speed increase because of gravity, ρ is the liquid thickness, ν is the kinematic thickness, , σ is the electrical conductivity of the liquid, α_1 is the material boundary, β is the warm development coefficient, β* is the volumetric extension coefficient, T, T_∞ is the temperature of the liquid inside the limit layer and the liquid temperature in the free stream individually while C, C_∞ are the relating species groupings of the liquid, κ is the warm conductivity of the liquid, c_p is the particular intensity at steady strain p, qr is the radiative intensity transition, D_{BM} is the Brownian movement factor, D_{TP} is the thermophoresis factor K_T is the warm dissemination proportion, Tm is the mean liquid temperature, k_r is the pace of substance response, $k_r>0$ addresses for damaging response, $k_r<0$ addresses for generative response and $k_r=0$ addresses for no response, $V_T=-\frac{k\nu}{T_r}\frac{\partial T}{\partial y}$ is the thermophoretic speed, where k is the thermophoretic coefficient and Tr is some reference temperature.

We assume the bottom surface of the plate is heated by convection from a hot fluid at temperature T_w which provides a heat transfer coefficient h_w. The boundary conditions of the present model are

$$\left.\begin{aligned}
&\mathrm{u}=u_w,\mathrm{v}=\mathrm{v}_0,-\kappa\frac{\partial \mathrm{T}}{\partial \mathrm{y}}=\mathrm{h}_w(\mathrm{T}_w-\mathrm{T}),C=C_w,\mathrm{M}=\mathrm{M}_W \text{ at } y=0,\\
&u\to 0,\ \frac{\partial u}{\partial x}\to 0,\mathrm{T}\to T_\infty,\ \mathrm{C}\to \mathrm{C}_\infty,\mathrm{M}\to \mathrm{M}_\infty \text{ as } y\to\infty
\end{aligned}\right\} \quad \text{.....(2)}$$

where v_0 is the suction/injection velocity.

Using the Rosseland approximation, the radiative heat flux term is given by

$$q_r = -\frac{4\sigma^*}{3k^*}\frac{\partial T^4}{\partial y} \quad \text{.....(3)}$$

where σ^* is the Stefan Boltzmann constant and k^* is the mean absorption coefficient. Assuming that the differences in temperature within the flow are such that T^4 can be expressed as a linear combination of the temperature, we expand T^4 in Taylor's series about T_∞ and neglecting higher order terms, we get

$$T^4 = 4T_\infty^3 T - 3T_\infty^4 \quad \text{.....(4)}$$

Thus, we have

$$\frac{\partial q_r}{\partial y} = -\frac{16T_\infty^3\sigma^*}{3k^*}\frac{\partial^2 T}{\partial y^2} \quad \text{.....(5)}$$

where σ* is the Stefan-Boltzmann constant and k* is the mean absorption coefficient.

Following the lines of Olajuwon [123], the similarity transformations as given below are introduced:

$$u = cxf'(\eta),\ v = -(c\nu)^{1/2} f(\eta),\ \theta(\eta) = \frac{T - T_\infty}{T_w - T_\infty},\ \phi(\eta) = \frac{C - C_\infty}{C_w - C_\infty},\ \chi(\eta) = \frac{M - M_\infty}{M_w - M_\infty}, \quad \text{.....(6)}$$

$$\text{where } \eta = \left(\frac{c}{\nu}\right)^{1/2} y \quad \text{.....(7)}$$

Use transformation (7), Equations. (2) reduces to the ordinary differential equations:

$$\left.\begin{aligned}
&f''' + ff'' - (f')^2 + \lambda_1(2ff'' - ff''') - Mf' + Gr.\theta + Gm.\phi = 0\\
&(1+N)\theta'' + Pr.f\theta' + Pr.Ec.\left\{\begin{aligned}&N_{BM}\theta'\phi' + N_{TP}(\phi')^2\\&+\lambda_1 f''(ff'' - ff''') + Mf'^2\end{aligned}\right\} = 0\\
&\phi'' + Sc.f\phi' + \frac{N_{BM}}{N_{TP}}\theta'' - Sc.Kr.\phi = 0\\
&\chi'' + Pr.Lb.f\chi' - Pe\{\chi'\phi' + (\chi+\beta)\phi''\} = 0
\end{aligned}\right\} \quad \text{.....(8)}$$

The boundary conditions (4.2) then turn into

$$\left.\begin{aligned}
&f(0) = f_s,\ f'(0) = 1, \theta'(0) = -\alpha(1 - \theta(0)), \phi(0) = 1, \chi(0) = 1\\
&f' \to 0,\ f'' \to 0, \theta \to 0, \chi \to 0 \text{ as } \eta \to \infty
\end{aligned}\right\} \quad \text{.....(9)}$$

Here prime denotes differentiation with respect to η, $\lambda_1 = \alpha_1 a/\rho\nu$ is the second grade fluid parameter, $M = \sigma B_0^2/\rho a$ is the magnetic field parameter, $f_s = v_0/(a\nu)^{1/2}$ is the suction parameter, $N = 16T_\infty^3\sigma^*/3k^*\kappa$ is the thermal radiation parameter, $Pr = \mu c_p/\kappa$ is the Prandtl number,

$\mathrm{Ec} = u_w{}^2/\mathrm{c_p}(\mathrm{T_w} - \mathrm{T_p})$ is the Eckert number, $N_{TP} = \frac{\tau D_{TP}(T_w - T_\infty)}{T_\infty \nu}$ is the thermophoresis parameter, $\mathrm{Sc} = \nu/\mathrm{D_m}$ is the Schmidt number, $N_{BM} = \frac{\tau D_{BM} C_\infty}{\nu}$ is the Brownian motion parameter, $\mathrm{Gr} = g\beta(\mathrm{T_w} - \mathrm{T_\infty})/a$ is the thermal Grashof number, $\mathrm{Gm} = g\beta^*(\mathrm{C_w} - \mathrm{C_\infty})/a$ is the solutal Grashof number, $\mathrm{Kr} = \mathrm{k_r}\nu/a\mathrm{D_m}$ is the chemical reaction parameter and $\alpha = h_w / \kappa(\nu/a)^{1/2}$ is the surface convection parameter, $Pe = \frac{bW_c}{D_{MO}}$ Peclet number for microorganisms, $Lb = \frac{\alpha}{D_{MO}}$ Lewis number for bioconvection, $\beta = \frac{M_\infty}{M_w - M_\infty}$ dimensionless microorganism density number.

The physical quantities of practical and engineering primary interest are the skin friction coefficient, Nusselt number and Sherwood number. The equation defining the wall shear stress is

4258

$$\tau_w = \left[\mu \frac{\partial u}{\partial y} + \rho\alpha_1 \left(2 \frac{\partial u}{\partial x}\frac{\partial u}{\partial y} + u \frac{\partial^2 u}{\partial x \partial y}\right) \right]_{y=0} \quad \text{.....(10)}$$

The local dimensionless skin friction coefficient is given by

$$\mathrm{C_f} = 2\mathrm{Re}^{-1/2}[1+3\lambda_1 f'(0)]f''(0)$$
$$\Rightarrow \mathrm{C_f^*} = \frac{1}{2}\mathrm{Re}^{1/2}\mathrm{C_f} = [1+3\lambda_1 f'(0)]f''(0) \quad \text{.....(11)}$$

Knowing the temperature field, it is interesting to study the effect of the free convection and thermal radiation on the rate of heat transfer q_w, is given by

$$q_w = -\kappa\left(\frac{\partial T}{\partial y}\right)_{y=0} - \frac{16T_\infty^3\sigma^*}{3k^*}\left(\frac{\partial^2 T}{\partial y^2}\right)_{y=0} \quad \text{.....(12)}$$

So, the rate of heat transfer in terms of dimensionless Nusselt number is defined as follows:

$$\mathrm{Nu} = -\mathrm{Re}^{1/2}(1+N)\theta'(0)$$
$$\Rightarrow \mathrm{Nu}^* = \mathrm{Re}^{-1/2}\mathrm{Nu} = -(1+Nr)\theta'(0) \quad \text{.....(13)}$$

Similarly, the rate of mass transfer in terms of dimensionless Sherwood number is given by

$$\mathrm{Sh} = -\mathrm{Re}^{1/2}\phi'(0)$$
$$\Rightarrow \mathrm{Sh}^* = \mathrm{Re}^{-1/2}\mathrm{Sh} = -\phi'(0) \quad \text{.....(14)}$$

And the rate of mass transfer of microorganisms is termed as

$$Mh = -\mathrm{Re}^{1/2}\chi'(0)$$
$$\Rightarrow Mh^{*} = \mathrm{Re}^{-1/2}\mathrm{Mh} = -\chi'(0) \quad \text{.....(15)}$$

3.

SOLUTION TECHNIQUES

To solve the set of equations under the boundary conditions , a numerical approach is employed. The Nachtsheim and Swigert shooting method, coupled with the Runge-Kutta sixth-order integration scheme, is used for the numerical analysis. The initial conditions for f''(0), θ(0), $\chi(0)$ and ϕ(0) are assumed and then numerically solved as an initial value problem. A step size of Δη = 0.005 is adopted to obtain numerical solutions with a tolerance level of 10^-6. It's worth noting that the Nachtsheim and Swigert shooting technique is a well-established method and has been successfully applied to solve various nonlinear fluid flow problems.

4259

Table 1: Comparison of -θ'(0) for various values of N

N	$-\theta'(0)$		
	Das [133]	Olajuwon [123]	Present Study
0.2	1.58882	1.59570	1.595722
0.5	1.72067	1.70501	1.705012
0.7	0.37381	0.37350	0.373517
2.0	2.67568	2.67560	2.675601
5.0	2.34861	2.35450	2.354531

To thoroughly validate the accuracy of the numerical code, the variations of -θ'(0) are examined for different values of $Pr = Ec = \alpha = 0$, and the results are presented in Table 1 The comparison between the outcomes obtained using the current code and those from the studies by Olajuwon [14] and Das [15] demonstrates excellent agreement. Hence, the employed numerical code for the present model can be confidently regarded as accurate.

4. STATISTICAL ANALYSIS

From Table 4, the producers have taken care of the coefficients of relationship (r) between the different critical pieces of the stream and certifiable totals and introduced them in Table 2. Here we can see that all the affiliation is tremendous as their qualities are

extraordinarily right around +1 or - 1. Comparably utilizing the information from Table 3, producers have overviewed the qualities coefficients of attestation (D=r2) in Table 4, which empowers us to check up the strength of affiliation and control of fitting variable of the stream on the certifiable aggregates.

It is seen that Brownian improvement influences skin pulverizing of the stream, while it altogether influences warmth and mass exchange cutoff of the stream. In any case, on the backwards thermophoresis vehemently influences skin contact at any rate unfavorable outcome on warmth and mass exchange of both nanoparticles and microorganisms. It is similarly seen that external appealing field has raises the general show of the stream system in all factors.

Table 2 : Values of physical quantities for various values of flow factors

N	α	λ_1	C_f^*	Nu^*	Sh^*	Mh^*
0.0			-5.6243	0.0601	0.7351	0.4526
0.4	0.1	2.0	-5.4905	0.0853	0.7446	0.4625
0.8			-5.4134	0.1112	0.7512	0.4711
	0.0		-5.6259	0.0000	0.7383	0.5612
0.2	0.5	2.0	-5.3172	0.3132	0.7398	0.5678
	2.0		-4.9201	0.7054	0.7423	0.5712
		2.0	-5.5535	0.0789	0.7358	0.4601
0.2	0.1	4.0	-9.1415	0.0663	0.7412	0.4721
		6.0	-12.6152	0.0548	0.7545	0.4803

4260

Table 3 : Correlation of Coefficients (r) between various factors with various physical quantities

r	C_f^*	Nu^*	Sh^*	Mh^*
N	-0.97584	0.96451	0.95114	0.98121
α	-0.96445	0.95471	0.96184	0.97112
λ_1	0.97884	-0.97551	0.97223	0.96884

Table 4 : Coefficients of Determinations (D) between various factors with various physical quantities

$D = r^2$	C_f^*	Nu^*	Sh^*	Mh^*
N	0.952264	0.93028	0.904667	0.962773
α	0.930164	0.911471	0.925136	0.943074
λ_1	0.958128	0.95162	0.945231	0.938651

5. RESULT AND DISCUSSIONS:

The numerical computations involve employing the procedure outlined in the previous section to analyze the flow characteristics of a second-grade fluid over a convectively heated expanding sheet for various parameter values. The results are visually presented in Figs. 2-10 and tabulated in Table 2. Multiple parameters are associated with the final version of the model. The problem can be extended along various dimensions; however, the initial focus appears to be on studying the impacts of surface convection parameter, radiation parameter, second grade parameter, and thermophoretic parameter. The default values of material parameters adopted in the simulation are M = 4.0, Sc = 0.64, λ1 = 1.5, a = 0.1, Gr = 5, Gm = 5, Pr = 0.71, N = 0.4, Ec = 0.02, Pe = 0.1, Lb = 1.0, and ß = 0.2, unless otherwise specified.

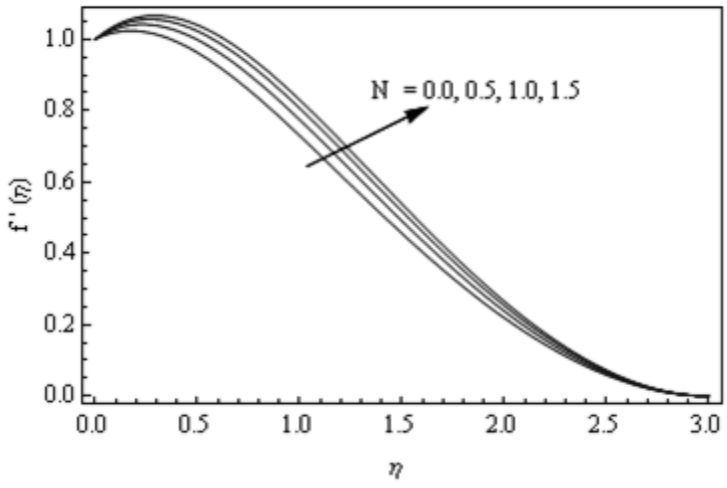

Figure 2: Velocity profiles for various values of N

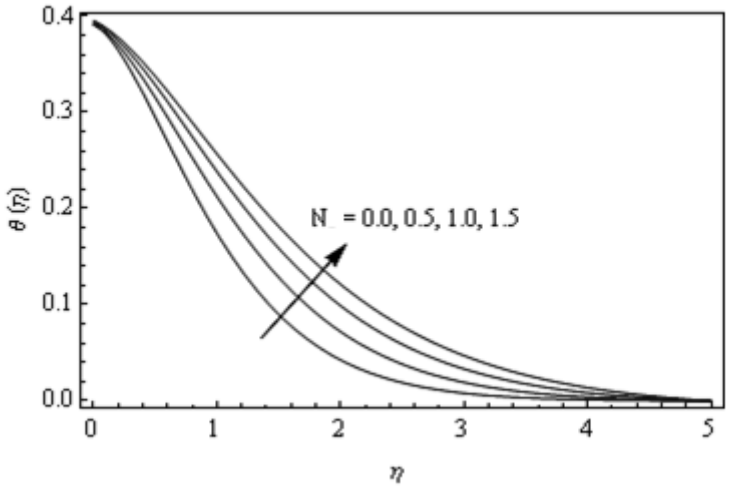

Figure 3 : Temperature profiles for various values of N

Figures 2-4 illustrate the behavior of velocity and temperature distribution for different values of the radiation parameter N. In Figure 2, it can be observed that an increase in the radiation parameter leads to an overall enhancement of fluid velocity within the boundary layer region. This phenomenon can be attributed to the fact that thermal radiation augments the thickness of the thermal boundary layer, subsequently influencing the velocity.

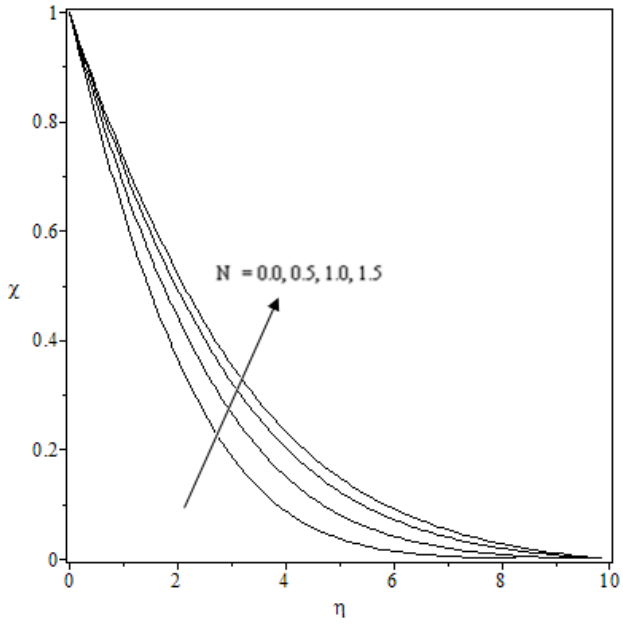

Figure 4 : Microorganism density profiles for various values of N

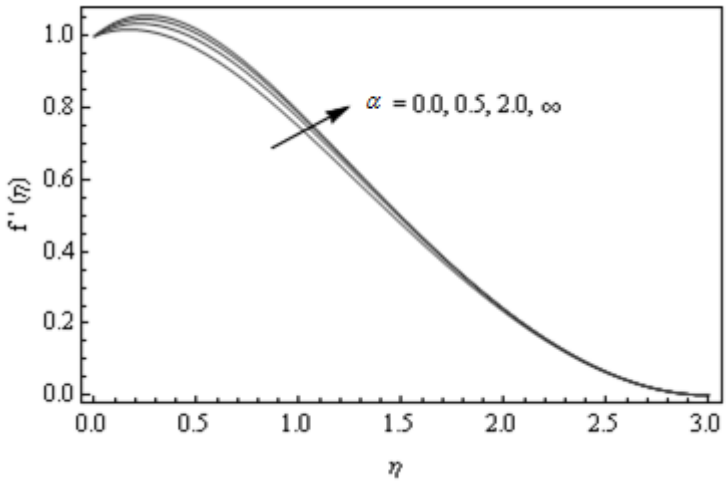

Figure 5 : Velocity profiles for various values of α

Figure 3 reveals another aspect, indicating a consistent rise in temperature distribution as the radiation parameter N increases. Consequently, elevating N leads to an enhancement in the thickness of the thermal boundary layer. Similar trends are observed in the case of microbial density, influenced by the parameter N. Table 2 further demonstrates that with an increase in the radiation parameter N, the reduced skin friction coefficient diminishes. However, concurrently, warm radiation enhances the rate of heat transfer.

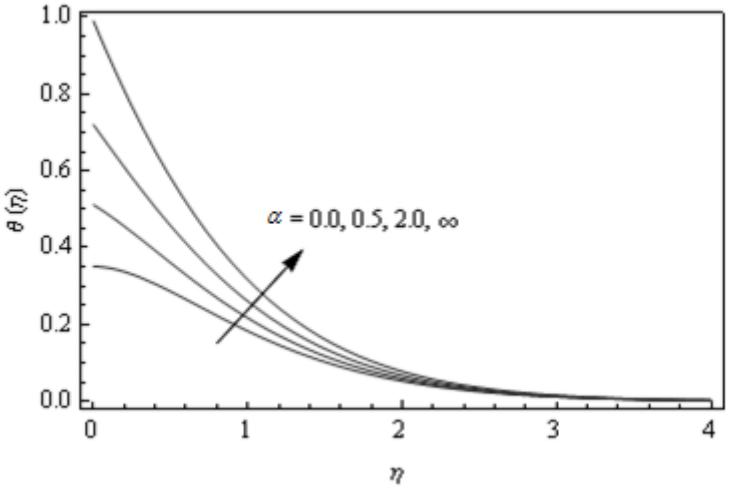

Figure 6: Temperature profiles for various values of α

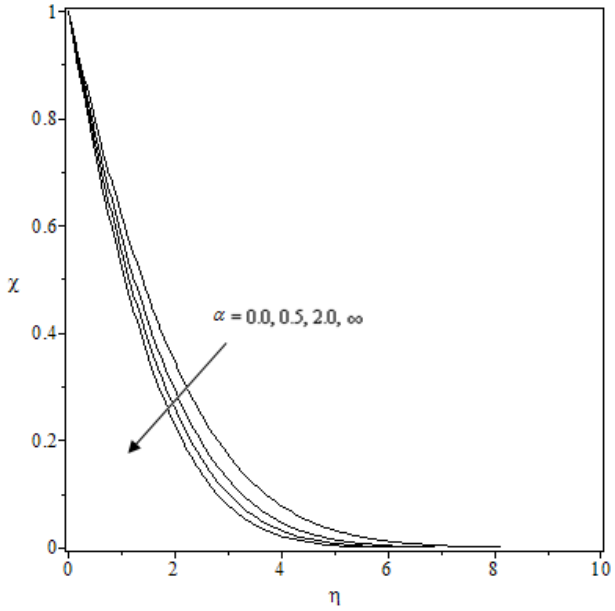

Figure 7 : Microorganism density profiles for various values of α

The effect of surface convection limit on the stream wise speed part is shown in Figure 5. As the value of constructs, the stream rate updates and as needs be achieving a development in the speed profiles as depicted in Figure 5. The impact of surface convection limit on fluid temperature in presence of warm radiation is displayed in Figure 6.

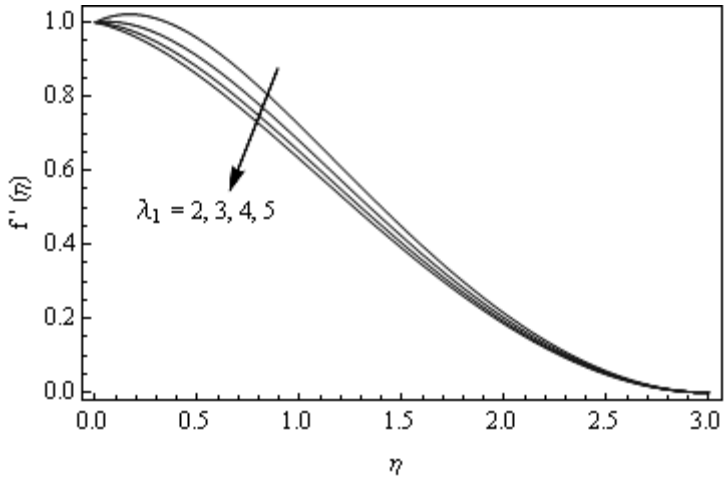

Figure 8 : Velocity profiles for various values of λ_1

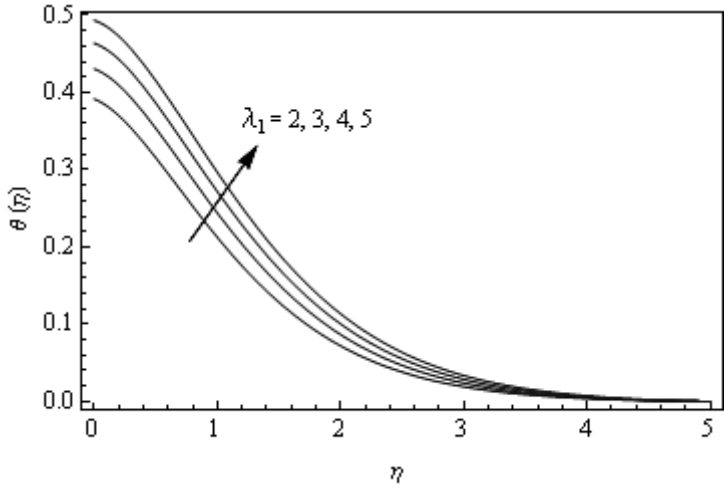

Figure 9 : Temperature profiles for various values of λ_1

In the figure, the augmentation of the thermal boundary layer region corresponds to an increase in fluid temperature. In the case of significant parameter values, such as (8), the solution converges to that of a constant surface temperature. The limit condition (9) highlights θ(0) = 1 as (8), validating the numerical findings of this study. Meanwhile, Figure 7 illustrates a reduction in microbial density with higher parameter values. Table 2 reveals that the heat transfer rate at the plate rises as ß increases, whereas the effect is converse for the wall shear stress at the plate. Specifically, the reduced skin friction coefficient decreases with an expansion of the surface convection parameter.

The influence of the second-grade parameter λ1 on fluid velocity and temperature distribution is depicted in Figures 8-10. Figure 8 clearly shows a decrease in velocity across the boundary layer with an increase in the second-grade parameter. This reduction asymptotically approaches zero at the boundary layer edge. As observed in Figure 9, an increment in the second-grade parameter leads to enhanced temperature profiles, consequently increasing the thickness of the thermal boundary layer. Similarly, Figure 10 displays an elevation in microbial density with higher values of the second-grade parameter.

Table 2 provides insight into the effects of increasing λ1: the reduced skin friction coefficient (in absolute terms) increases, while the reduced Nusselt number decreases.

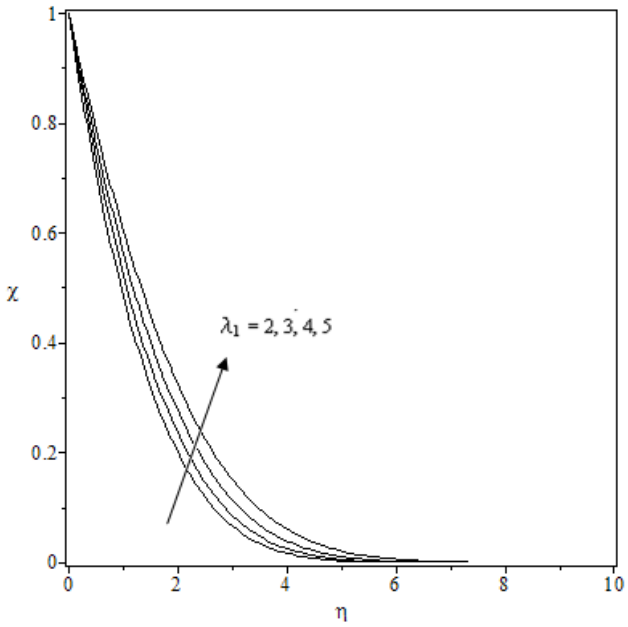

Figure 10 : Microorganism density profiles for various values of λ_1

6. CONCLUDING REMARKS

The current investigation concentrates on the effects of thermophoresis and Brownian motion on the magnetohydrodynamic (MHD) boundary layer flow of a second-grade fluid over an expanding sheet with convective surface force progression and the presence of gyrotactic microorganisms.

Through proper similarity transformations, th e governing equations are converted into a se t of ordinary differential equations, which are then numerically solved.

The collected findings are displayed in the for m of graphs and tables, which highlight the flo w characteristics and show how they depend on the properties of the material.

The conclusions drawn from this study can be summarized as follows:

- Higher warm radiation and surface conv ection parameter values result in an inc rease in fluid velocity within the bounda ry layer region, but thermophoretic and second-
  grade parameters have the reverse imp act.
- Elevated warm radiation, second grade parameter, and surface convection parameter values improve temperature profiles.
- The presence of thermophoresis reduces t he concentration of chemical species, incr easing the rate of mass transfer that is go verned by the thermophoretic parameter.
- The magnitude of the skin friction coeffici ent reduces as warm radiation and surfac e convection parameters are increased, b ut the tendency for thermophoretic and s econd- grade parameters is the opposite.
- While the rate of heat transfer reduces with rising values of the second-grade parameter, it increases with greater values of the surface convection and warm radiation parameters.

7. REFERENCES :

[1] Yih, K.A., 1999. MHD forced convection flow adjacent to a non-isothermal wedge. International Communications in Heat and Mass Transfer, 26(6), pp.819-827.

[2] Guell, D.C., Brenner, H., Frankel, R.B. and Hartman, H., 1988. Hydrodynamic forces and band formation in swimming magnetotactic bacteria. Journal of theoretical Biology, 135(4), pp.525-542.

[3] Hillesdon, A.J., Pedley, T.J. and Kessler, J.O., 1995. The development of concentration gradients in a suspension of chemotactic bacteria. Bulletin of mathematical biology, 57, pp.299-344.

[4] Ishikawa, T., Simmonds, M.P. and Pedley, T.J., 2006. Hydrodynamic interaction of two swimming model micro-organisms. Journal of Fluid Mechanics, 568, pp.119-160.

[5] Mehandia, V. and Nott, P.R., 2008. The collective dynamics of self-propelled particles. Journal of Fluid Mechanics, 595, pp.239-264.

[6] Kuznetsov, A.V., 2011. Bio-thermal convection induced by two different species of microorganisms. International Communications in Heat and Mass Transfer, 38(5), pp.548-553.

[7] Jayachandra Babu, M., Sandeep, N. and Raju, C.S., 2016. Heat and mass transfer in MHD Eyring-Powell nanofluid flow due to cone in porous medium. In International Journal of Engineering Research in Africa (Vol. 19, pp. 57-74). Trans Tech Publications Ltd.

[8] Ur-Rehman, S., Nadeem, S. and Lee, C., 2016. Series solution of magneto-hydrodynamic boundary layer flow over bi-directional exponentially stretching surfaces. Journal of the Brazilian Society of Mechanical Sciences and Engineering, 38(2), pp.443-453.

[9] Hussain, S.T., Khan, Z.H. and Nadeem, S., 2016. Water driven flow of carbon nanotubes in a rotating channel. Journal of Molecular Liquids, 214, pp.136-144.

[10] Akbar, N., Khan, Z., Nadeem, S. and Khan, W., 2016. Double-diffusive natural convective boundary-layer flow of a nanofluid over a stretching sheet with magnetic field. International Journal of Numerical Methods for Heat & Fluid Flow, 26(1), pp.108-121.

[11] Raju, C.S.K. and Sandeep, N., 2016. Falkner-Skan flow of a magnetic-Carreau fluid past a wedge in the presence of cross diffusion effects. The European Physical Journal Plus, 131, pp.1-13.

[12] Hussain, S.T., Nadeem, S. and Qasim, M., 2016. Impact of linear operator on the convergence of HAM solution: a modified operator approach. Advances in Applied Mathematics and Mechanics, 8(3), pp.499-516.

[13] Nadeem, S., Khan, A.U. and Saleem, S., 2016. A comparative analysis on different nanofluid models for the oscillatory stagnation point flow. The European Physical Journal Plus, 131, pp.1-14.

[14] Olajuwon, B.I.: Convection heat and mass transfer in a hydromagnetic flow of a second grade fluid in the presence of thermal radiation and thermal diffusion. Int Comm Heat Mass Trans 38, 377-382 (2011).

[15] Das, K.: Influence of chemical reaction and viscous dissipation on MHD mixed convection flow. Jour Mech Sci and Tech. 28 (5) 1881-1885 (2014).